

Numerical Simulations of Spontaneous Ignition of Mono-disperse Fuel Spray in Lean Premixed Gas

O. Moriue*, Y. Kawaida, H. Kato and E. Murase

Department of Mechanical Engineering

Kyushu University

Motooka 744, Nishi-ku, 8190395 Fukuoka, Japan

Abstract

Spontaneous ignition of mono-disperse fuel spray with uniform droplet distribution in hot fuel/air premixed gas was simulated through one-dimensional numerical model of an isolated fuel droplet in a closed constant-volume cell. Namely, the inter-droplet interaction in a spray was expressed through the interference of the outer boundary of the cell. Equivalence ratio calculated from initial amounts of fuel in the liquid phase and oxygen in the gas phase was defined as liquid-phase equivalence ratio ϕ_l . Since the premixed gas was fuel-lean, the existence of the droplet might either promote the ignition through a role as fuel source or hinder the ignition through a role as heat sink, which could depend on initial droplet diameter d_0 , ϕ_l , initial gas-phase temperature T_{g0} , initial liquid-phase temperature T_{l0} , gas-phase equivalence ratio ϕ_g and initial pressure P_0 . The effects of the first three conditions were examined. d_0 was less than 200 μm and typically around 30 μm . T_{l0} , ϕ_g and P_0 were 300 K, 0.4 and 3 MPa, respectively. Fuel was *n*-heptane. Detailed chemical kinetics including the low-temperature oxidation reactions were employed, and therefore cool-flame ignition delay τ_{cf} and hot-flame ignition delay τ_{ig} were evaluated. First, only d_0 was varied. When d_0 was relatively large, both τ_{cf} and τ_{ig} were not different from those of only premixed gas with the same ϕ_g . It means that such large droplet required relatively long time for vaporization compared with chemical characteristic time, and the ignition occurred at the outer boundary of the cell that the fuel vapor from the droplet did not reach. However, as d_0 decreased, τ_{cf} and τ_{ig} increased and decreased, respectively, first. Thus interaction between spray and premixed gas was recognized. Next, only ϕ_l was varied. With increasing ϕ_l , τ_{ig} either increased monotonically or had minimal value depending on T_{g0} .

Introduction

Spontaneous ignition of fuel spray in hot ambient gas is a research subject related to many practical combustion devices for which liquid fuel is utilized like diesel engines. In order to increase efficiency and reduce pollutional emissions of such combustion devices, it is important to obtain ignition characteristics of sprays systematically according to ambient-gas conditions and spray characteristics. An isolated fuel droplet has been studied as the simplest model of sprays [1-6]. Through such studies, systematic knowledge of the single-droplet ignition has been obtained. However, they treated a droplet in an open space, and therefore the droplet had ignitable limit in terms of initial droplet diameter [1, 2]. Thus there was a gap between sprays and isolated droplets. The authors developed the numerical model that simulates a droplet placed in a constant-volume cell that is closed against mass and energy transport [7]. Thus the inter-droplet interaction in a spray was expressed through the interference of the outer boundary of the cell, and mono-disperse fuel spray with uniform droplet distribution was simulated through the model. The authors studied mono-disperse spray in hot air composed of fine droplets whose diameters were less than 100 μm , which would not have ignited if they had been in an open space. In the study, overall equivalence ratio ϕ_{overall} was defined as the equivalence ratio in the cell after the complete vaporization of the droplet without reactions, which depends on the ratio of the cell diameter to the initial droplet diameter d_0 , initial gas-phase temperature T_{g0} , initial liquid-phase temperature T_{l0} and initial pressure P_0 , and the effects of d_0 and ϕ_{overall} on the ignition characteristics were revealed.

In the present study, the composition of the ambient gas was varied, and the spontaneous ignition of mono-disperse fuel spray in hot fuel/air premixed gas was numerically simulated. Liquid-phase equivalence ratio ϕ_l should be newly defined as the equivalence ratio calculated from initial amounts of fuel in the liquid phase and oxygen in the gas phase. When the ambient gas had been air, ϕ_{overall} would have been equal to ϕ_l . However, since the ambient

*Corresponding author

gas was premixed gas, ϕ_{overall} was the sum of ϕ and initial gas-phase equivalence ratio ϕ_g . ϕ_g was smaller than unity and large enough so that the premixed gas could have ignited without the spray. Since the premixed gas was fuel-lean, the existence of the spray might either promote the ignition through a role as fuel source or hinder the ignition through a role as heat sink, which could depend on d_0 , ϕ , T_{g0} , T_{l0} , ϕ_g and P_0 . The effects of the first three conditions were examined in the present study. It is well known that the low-temperature oxidation reactions are dominant for the spontaneous ignition of most hydrocarbon fuels. The low-temperature oxidation reactions are suppressed when the temperature exceeds around 800-1000 K, and consequently cool flame appears, which has relatively low flame temperature compared with hot flame, which is induced by the high-temperature oxidation reactions. For the spontaneous ignition of such hydrocarbons, two-stage ignition occurs, namely, the cool-flame appearance and the subsequent hot-flame appearance [5]. To analyze such ignition process, cool-flame ignition delay τ_{cf} and hot-flame ignition delay τ_{ig} were evaluated.

Model Description

The model simulated the spontaneous ignition of a cold fuel droplet placed in hot and quiescent ambient gas. A spherical droplet was positioned at the center of a closed spherical cell with a constant volume, and one-dimensional calculation was done with spherical symmetry. The model was transient and based on mass, species and energy conservations. Momentum conservation was neglected, and pressure P was treated as spatially uniform and time-dependent. The boundary conditions at the outer boundary of the cell were chosen so that the cell was closed against mass and energy transport. Vaporization of the fuel and regression of the droplet surface were implicitly calculated from fugacity equilibrium and mass- and energy-flux continuities at the droplet surface. Linear grid arrangement was employed in the liquid phase, and exponential in the gas phase, which was fixed at the droplet surface and at the outer boundary of the cell. The numbers of the grid points were varied depending on the conditions, and were typically 21 and 81 in the liquid and gas phases, respectively. Spatial discretization was done with the second order central difference scheme, and temporal discretization was with implicit multi-order backward differentiation method. Dependent variables of the system were mass fraction of each species Y_i , temperature T , P and droplet radius R . The first two variables were the functions of independent variables of time t and radial coordinate r , and the last two variables were the function of t . Initially there was no gradient in Y_i and T except at the droplet surface, and velocity was zero at all the grid points. The model could continue calculation even after the complete vaporization of the droplet. When the droplet diameter became smaller than the certain value that was small enough, the droplet diameter was held to be constant, and the same boundary conditions as those at the outer boundary of the cell were applied at the droplet surface. Fuel in the liquid phase and in the premixed gas was both *n*-heptane. Detailed chemical kinetics with 437 reactions and 92 species was employed, which can reproduce the two-stage ignition behavior. The details of the model are described in the previous study [7]. The model was one-dimensional, and neither the slip between the droplet and the ambient gas nor the macroscopic behavior of the spray could be considered. Thus there was still a gap between the modeled spray and the real spray. The investigation was nevertheless carried out in order to obtain fundamental ignition characteristics based on detailed chemistry.

In the present study, T_{l0} , ϕ_g and P_0 were fixed to 300 K, 0.4 and 3 MPa, respectively. ϕ depends on the ratio of the cell diameter to d_0 , T_{g0} , T_{l0} , ϕ_g and P_0 . With the last three conditions already fixed, when d_0 and T_{g0} were fixed, ϕ had a one-to-one correlation with the ratio of the cell diameter to d_0 , namely, with droplet number density in the spray.

Results and Discussion

A typical example of the spontaneous ignition process is shown in Fig. 1. The figure shows the history of the maximum temperature among all the grid points T_{max} for $T_{g0} = 800$ K, $\phi = 0.4$ and $d_0 = 40$ μm . The two-stage ignition behavior is obviously recognized. In the present study, the moment of hot-flame ignition was defined as the moment when the maximum value of the temperature rise rate derived from chemical reactions $(\partial T / \partial t)_{\text{ch}}$ among all the grid points exceeded 10^7 K/s. The moment of cool-flame ignition was defined as the moment when any of the temperature rise rate derived from chemical reactions $(\partial T / \partial t)_{\text{ch}}$ at each grid point took a temporal maximal value. With these definitions, τ_{cf} and τ_{ig} were evaluated, and both ignition delays in this case are also shown in Fig. 1. Figure 1 does not provide the information on the radial direction. Figure 2 shows the transition of the distribution of $(\partial T / \partial t)_{\text{ch}}$ for the same conditions as those for Fig. 1. The origin of the abscissa corresponds to the droplet center, and the initial location of the droplet surface is 0.02 mm. The outer boundary of the cell is around 0.251 mm though it is over the range shown in the figure. The legends show the time. The time "0.351 ms" corresponds to the moment of cool-flame ignition. It is observed that cool flame appeared first around the outer boundary of the cell. It means that

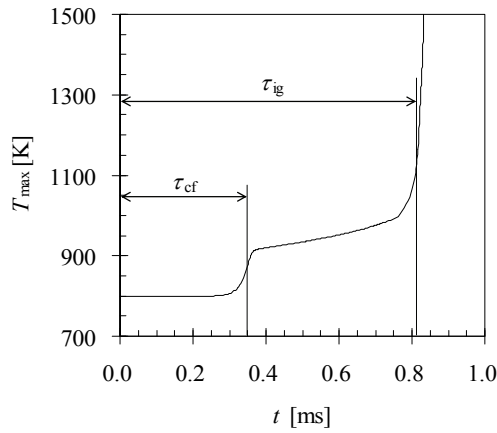


Figure 1. History of maximum temperature T_{\max} .
 $P_0=3$ MPa, $T_{g0}=800$ K, $\phi_g=0.4$, $\phi_l=0.4$, $d_0=40$ μm

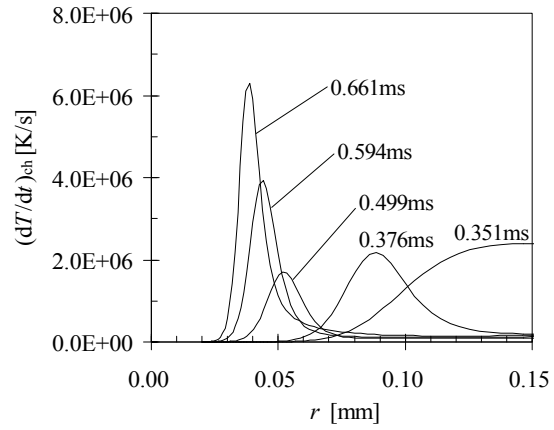


Figure 2. Transition of distribution of chemical-reaction-derived temperature rising rate $(dT/dt)_{\text{ch}}$.
 $P_0=3$ MPa, $T_{g0}=800$ K, $\phi_g=0.4$, $\phi_l=0.4$, $d_0=40$ μm

the role as heat sink of the droplet prevailed over its role as fuel source for the low-temperature oxidation reactions. The reaction region then shifted inward to the droplet, where fuel had not reacted yet. Because of higher fuel concentration near the droplet, the reactions became more active (0.594 ms and 0.661 ms). The active reactions in this region led to hot-flame appearance in the same region though the moment of hot-flame appearance is not shown in the figure.

The effect of d_0 was first examined. Dependences of τ_{cf} and τ_{ig} on d_0 for the case of $T_{g0} = 800$ K and $\phi_l = 0.4$ are shown in Fig. 3. The minimum d_0 calculated was 1 μm . τ_{cf} and τ_{ig} of only premixed gas with the same P_0 , T_{g0} and ϕ_g are also shown for reference by straight lines, which are expressed as "no spray" in the legends. The effect of the existence of the spray on the ignition process depends on d_0 . When d_0 is relatively large (over 80 μm), both τ_{cf} and τ_{ig} are not different from those of the only premixed gas. It means that such large droplet required relatively long time for vaporization compared with chemical characteristic time, and the boundary layers of fuel concentration and temperature caused by the droplet did not reach the outer boundary of the cell before hot-flame appearance. (Note that the cell diameter is proportional to d_0 , since ϕ_l is fixed.) Therefore, the conditions around the outer boundary of the cell were not very different from those of the only premixed gas, and both cool flame and hot flame appeared there. However, as d_0 decreases, τ_{cf} increases, and τ_{ig} decreases, first. This tendency can be explained from the above

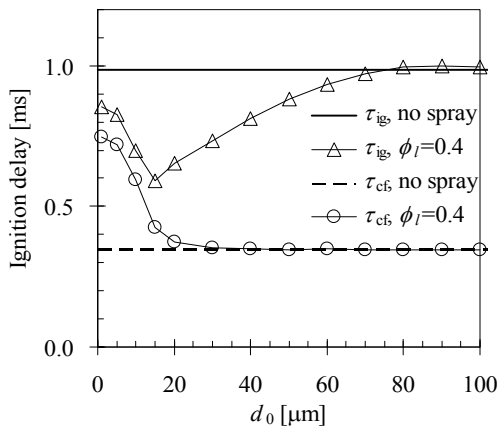


Figure 3. Dependences of cool-flame ignition delay τ_{cf} and hot-flame ignition delay τ_{ig} on initial droplet diameter d_0 .
 $P_0=3$ MPa, $T_{g0}=800$ K, $\phi_g=0.4$, $\phi_l=0.4$

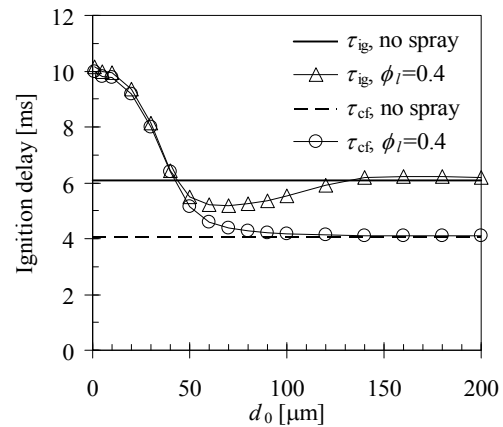


Figure 4. Dependences of cool-flame ignition delay τ_{cf} and hot-flame ignition delay τ_{ig} on initial droplet diameter d_0 .
 $P_0=3$ MPa, $T_{g0}=700$ K, $\phi_g=0.4$, $\phi_l=0.4$

discussion about Fig. 2, where d_0 was 40 μm . The cooling effect of the droplets hindered the low-temperature oxidation reactions to be activated and lengthened τ_{cf} . (Note that smaller droplet vaporizes faster.) Cool flame appeared around the outer boundary of the cell, where local temperature was the highest, and then propagated inward. Because of larger local equivalence ratio near the droplet, cool-flame temperature there was higher than that in the case of the only premixed gas. Higher cool-flame temperature led to shorter hot-flame induction time after cool-flame appearance ($\tau_2 = \tau_{\text{ig}} - \tau_{\text{cf}}$). This extent was more than that of the increase in τ_{cf} , and as the result τ_{ig} was shorter. As d_0 decreases further, τ_{ig} takes a minimum value and then increases. This is because the extent of the increase in τ_{cf} prevailed over that of the decrease of τ_2 . It was already reported in the previous study in which the ambient gas was air that τ_{ig} takes a minimum value at a certain d_0 [7]. Thus this is not peculiar to the case where ambient gas is premixed gas, and can be explained by the counteracting effects of the droplet, namely, fuel provision and cooling. As d_0 decreases further to zero, both τ_{cf} and τ_{ig} approach to the respective values. The origin of the abscissa corresponds to the premixed gas without spray with higher equivalence ratio ($= \phi_g + \phi$) and lower P_0 and T_{g0} (equilibrium values after mixing of the droplet and the ambient premixed gas without reactions). τ_{ig} at $d_0 = 0$ is shorter than that of the only ambient premixed gas in Fig. 3. Figure 4 shows the dependences of τ_{cf} and τ_{ig} on d_0 for the case of $T_{g0} = 700$ K. The other conditions are the same as those of Fig. 3. In this case, τ_{ig} at $d_0 = 0$ is longer than that of the only ambient premixed gas. Thus it depends on the conditions whether τ_{ig} at $d_0 = 0$ is shorter or longer than that of the only ambient premixed gas, namely, whether the increase in equivalence ratio prevails over the decrease in initial pressure and temperature for premixed-gas ignition. Other tendencies of Fig. 3 are basically the same as those of Fig. 4.

Next, the effect of ϕ was examined. Dependences of τ_{cf} and τ_{ig} on ϕ for the case of $T_{g0} = 800$ K and $d_0 = 30$ μm are shown in Fig. 5. τ_{cf} and τ_{ig} of only ambient premixed gas with the same P_0 , T_{g0} and ϕ_g are also shown for reference like in Figs. 3 and 4. As mentioned in Model Description, the abscissa can be also interpreted as droplet number density of the spray. Please note that $\phi = 0$ of the spray case does not correspond to the only ambient premixed gas. Instead it denotes an isolated droplet in an open space, namely, in the cell with infinite volume. Both τ_{cf} and τ_{ig} increase with increasing ϕ . The increase in droplet number density simply hinders the ignition. In a macroscopic view, higher droplet number density leads to lower energy density of the system composed of the spray and the premixed gas as well as to larger overall equivalence ratio ϕ_{overall} . The former effect is negative for the ignition from a physical aspect through longer droplet vaporization time. From a chemical aspect, it might depend on the conditions considering negative-temperature-coefficient temperature region of premixed gases. The latter effect is positive when ϕ_{overall} is less than unity at least, namely, when ϕ is less than 0.6 in this case. (Actually, this value should be much larger considering the inhomogeneity of the system.) As the result of all these effects, the increase in droplet number density monotonically delayed both cool- and hot-flame ignitions. For all ϕ , cool flame appeared at the outer boundary of the cell. This can be recognized from that τ_{cf} of an isolated droplet ($\phi = 0$) coincides with that of the only premixed gas. Figure 6 shows the dependences of τ_{cf} and τ_{ig} on ϕ for the case of $T_{g0} = 1000$ K. The other

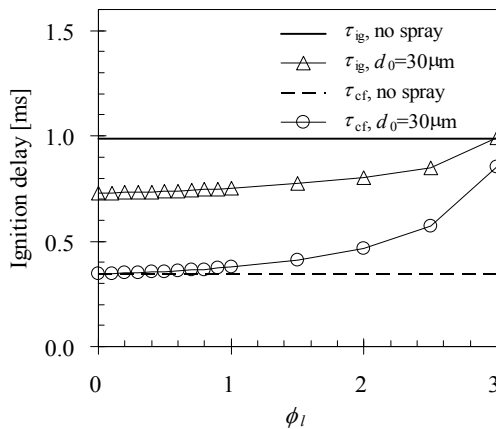


Figure 5. Dependences of cool-flame ignition delay τ_{cf} and hot-flame ignition delay τ_{ig} on liquid-phase equivalence ratio ϕ .
 $P_0 = 3$ MPa, $T_{g0} = 800$ K, $\phi_g = 0.4$, $d_0 = 30$ μm

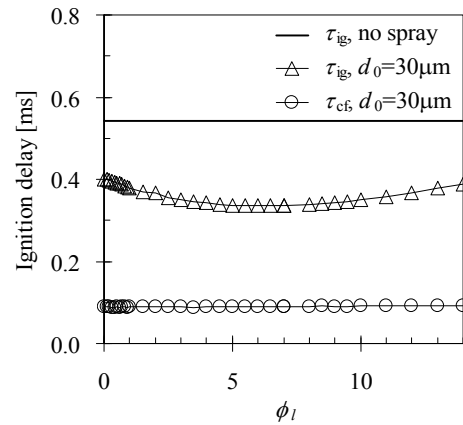


Figure 6. Dependences of cool-flame ignition delay τ_{cf} and hot-flame ignition delay τ_{ig} on liquid-phase equivalence ratio ϕ .
 $P_0 = 3$ MPa, $T_{g0} = 1000$ K, $\phi_g = 0.4$, $d_0 = 30$ μm

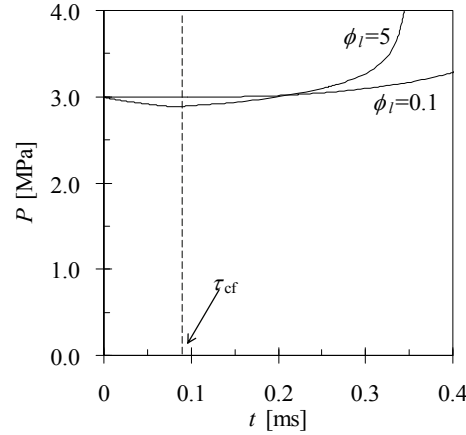


Figure 7. History of pressure P for different liquid-phase equivalence ratios ϕ_l .
 $P_0=3$ MPa, $T_{g0}=1000$ K, $\phi_g=0.4$, $d_0=30$ μm

conditions are the same as those of Fig. 5. In this case, only τ_{ig} is displayed for the only premixed gas, since no cool flame appeared for it. The initial temperature 1000 K is higher than the temperature range where the low-temperature oxidation reactions are active. When the spray existed, cool flame could appear because of the cooling effect of the spray. It means that cool flame appeared in the vicinity of each droplet unlike the case of Fig. 5. τ_{cf} depended on ϕ_l very little in the examined range. This is supposed to be because the time required to cool down the gas near the droplet depended on ϕ_l very little. τ_{ig} took a minimum value around $\phi_l = 5-7$. Since τ_{cf} is almost constant, this can be explained by the dependence of τ_2 on ϕ_l . First, the negative dependence of τ_2 on ϕ_l in the relatively small ϕ_l range is discussed. Since cool flame appeared only in the vicinity of each droplet, larger droplet number density leads to larger heat release by cool flame averaged per unit volume of the system assumed that the heat release per each droplet did not much depend on droplet number density. This is recognized in Fig. 7, which shows history of P for $\phi_l = 0.1$ and 5. Before the cool-flame appearance, P for $\phi_l = 5$ was smaller because of larger cooling effect of the spray. However, after the cool-flame appearance, pressure rise rate for $\phi_l = 5$ was larger, and finally P for $\phi_l = 5$ exceeded that for $\phi_l = 0.1$. Higher pressure activated the high-temperature oxidation reactions more, and then τ_2 was shorter. When ϕ_l is relatively large in Fig. 6, τ_2 increases as ϕ_l increases. This is simply because the cooling effect of the spray prevailed and because ϕ_{overall} was too large. The example that τ_{ig} takes a minimum value at a certain ϕ_l was already reported for the case of $\phi_g = 0$ in the previous study [7]. However, d_0 was much smaller (10 μm) in that case, and the ignition occurred long after the complete vaporization of the droplet. It was actually the ignition of homogeneous premixed gas unlike the case of Fig. 6. The fact that τ_{ig} takes a minimum value at a certain ϕ_l for spray ignition is supposed to be peculiar to the case where ambient gas is premixed gas. It is still unclear whether this is peculiar to the fuels that show the two-stage ignition behavior, and to be examined in the further study.

Conclusions

Spontaneous ignition of mono-disperse n -heptane spray with uniform droplet distribution in hot n -heptane/air premixed gas was numerically simulated through a one-dimensional model. Initial gas-phase equivalence ratio ϕ_g was 0.4 so that the ambient gas was fuel-lean and could have ignited without the spray. The effects of initial droplet diameter d_0 and liquid-phase equivalence ratio ϕ_l on the two-stage ignition process of the system were investigated for different initial gas-phase temperatures T_{g0} . Initial pressure P was 3 MPa. First, d_0 was varied with other conditions fixed ($\phi_l = 0.4$). When d_0 was relatively large, the droplet required relatively long time for vaporization compared with chemical characteristic time, and the ignition proceeded at the location that fuel vapor from the droplet did not reach. Therefore, both cool-flame ignition delay τ_{cf} and hot-flame ignition delay τ_{ig} were not different from those of the only ambient gas without the spray. When d_0 was relatively small, τ_{cf} increased with decreasing d_0 because of the cooling effect of the droplet. Cool flame, which appeared at the location farthest from the droplet, propagated inward to the droplet and activated hot flame in the vicinity of the droplet. τ_{ig} took a minimum value at a certain d_0 because of the counteracting roles of the droplet: fuel source and heat sink. Next, ϕ_l was varied with other conditions fixed ($d_0 = 30$ μm). When T_{g0} was 800 K, τ_{ig} increased monotonically with increasing ϕ_l . When T_{g0} was

1000 K, which is higher than the temperature range where the low-temperature oxidation reactions are active, τ_{ig} had minimal value at a certain ϕ . This was explained through the heat release by cool flame yielded limitedly in the vicinity of each droplet. The role of the spray in the spontaneous ignition of the system composed of the spray and the premixed gas depends on many conditions complicatedly. Further investigation is required.

Nomenclature

d	droplet diameter
P	pressure
r	radial coordinate
R	droplet radius
t	time
T	temperature
Y	mass fraction
τ_{cf}	cool-flame ignition delay
τ_{ig}	hot-flame ignition delay
ϕ	equivalence ratio

Subscripts

0	initial state
ch	derived from chemical reactions
g	gas-phase
i	species i
l	liquid-phase
max	spatially maximum value

References

1. Saitoh, T., Ishiguro, S. and Niioka, T., *Combust. Flame*, 48, pp. 27-32 (1982).
2. Tsukamoto, T., Okada, H. and Niioka, T., *Trans. Japan Soc. Aero. Space Sci.*, 35 (110), pp. 165-176 (1993).
3. Takei, M., Tsukamoto, T. and Niioka, T., *Combust. Flame*, 93, 149-156 (1993).
4. Bergeron, C. A. and Hallett, W. L. H., *The Canadian Journal of Chemical Engineering*, 67, 142-149 (1989).
5. Tanabe, M., Bolik, T., Eigenbrod, C., Rath, H. J., Sato, J. and Kono, M., *Proc. Combust. Inst.*, 26, pp. 1637-1643 (1996).
6. Schnaubelt, S., Moriue, O., Eigenbrod, C. and Rath, H. J., *Proc. Combust. Inst.*, 28, pp. 953-960 (2000).
7. Moriue, O., Mikami, M., Kojima, N. and Eigenbrod, C., *Proc. Combust. Inst.*, 30, pp. 1973-1980 (2005).